CHEMISTRY OF MATERIALS
Article

Chem. Mater. **2010,** *22,* 2041–2049 2041
DOI:10.1021/cm903270d

Fabrication, Characterization, and Electrical Properties of Langmuir−Blodgett Films of an Acid Terminated Phenylene−Ethynylene Oligomer

Ana Villares,[†] Gorka Pera,[†,‡] Santiago Martín,[†,§] Richard J. Nichols,[§] Donocadh P. Lydon,[⊥] Lucas Applegarth,[⊥] Andrew Beeby,[⊥] Paul J. Low,[⊥] and Pilar Cea*[,†,‡]

[†]*Departamento de Química Orgánica y Química Física, Facultad de Ciencias, Universidad de Zaragoza, 50009, Spain,* [‡]*Instituto de Nanociencia de Aragón (INA), Edificio i+d. Campus Rio Ebro, Universidad de Zaragoza, C/Mariano Esquillor, s/n, 50017 Zaragoza, Spain,* [§]*Department of Chemistry, University of Liverpool, Crown Street, Liverpool, L69 7ZD, United Kingdom, and* [⊥]*Department of Chemistry, University of Durham, Durham DH1 3LE, United Kingdom.*

Received October 25, 2009. Revised Manuscript Received January 13, 2010

This paper describes the preparation of Langmuir−Blodgett (LB) films comprised of an oligomeric phenylene−ethynylene (OPE) derivative, 4-[4-(phenylethynyl)-phenylethynyl] benzoic acid (BPEBA). Analysis of the surface pressure and surface potential vs area per molecule isotherms reveal that good quality monolayer films can be formed at surface pressures of 15 mN/m. The monolayers were transferred onto solid substrates with a Z-type deposition and a transfer ratio of 1. Raman and surface-enhanced Raman spectroscopy (SERS) studies reveal that the films are physisorbed onto silver metal substrates. The morphology of the deposited films was analyzed by means of atomic force microscopy (AFM), revealing the formation of homogeneous layers free of three-dimensional defects. The optical and emissive properties of the LB films were determined, with significant blue-shifted absorption spectra indicating the formation of two-dimensional H aggregates in the films. In addition, a significant Stokes shift in the excitation and emission spectra of the films is indicative of a distribution of molecular conformations around the long molecular axis in the solidlike monolayer environment. Scanning tunneling microscopy (STM) studies of single layer BPEBA LB films were performed. The tip−sample distance has been calibrated carefully to obtain $I-V$ curves above the LB film. $I-V$ curves are unexpectedly symmetrical in spite of the asymmetric contacts of the molecule with the tip and the substrate. Single molecule conductance for BPEBA has also been determined and the similarity of these results to $I-V$ data for BPEBA incorporated in LB films indicates that lateral (intermolecular) conductance is negligible for electrical measurements using the STM configuration.

Introduction

The field of conducting polymers has been a source of a vast body of new science,[1−5] and the number of new conducting and semiconducting polymeric materials employed in the fields of electronics and optoelectronics has rapidly increased due to the possibility of modulating the final properties with subtle modifications in the chemical structure. In contrast to the use of polymeric materials, which function through the electronic properties of the bulk, the field of molecular electronics arises from the use of single molecules to perform a certain task; therefore, the functionality is already present in the smallest component of the device.[6,7]

In recent times, a wide variety of novel electronically active, molecule-based devices have been proposed, and in some cases tested, for collecting, processing, displaying, and storing information.[8] The realization of a truly molecular electronic device relies upon the assembly of small packets of active molecules to build up a nanoscale device. This methodology, known as the "bottom-up approach", is commonly used in the fabrication of molecular electronic devices and test beds. Consequently, the development of molecular electronic technology has been closely related to the advances in synthetic chemistry, which provides access to the new molecular building

*Corresponding author. E-mail: pilarcea@unizar.es.

(1) Murphy, J.; Roubinek, L.; Wassermann, A. *J. Am. Chem. Soc.* **1961**, 1964.
(2) MacDiarmid, A. G. *Angew. Chem., Int. Ed.* **2001**, *40*(14), 2581.
(3) Argun, A. A.; Aubert, P. H.; Thompson, B. C.; Schwendeman, I.; Gaupp, C. L.; Hwang, J.; Pinto, N. J.; Tanner, D. B.; MacDiarmid, A. G.; Reynolds, J. R. *Chem. Mater.* **2004**, *16*(23), 4401.
(4) Shirakawa, H. *Angew. Chem., Int. Ed.* **2001**, *40*(14), 2575.
(5) Lee, K.; Cho, S.; Park, S. H.; Heeger, A. J.; Lee, C. W.; Lee, S. H. *Nature* **2006**, *441*(7089), 65.
(6) Ashwell, G. J. *Molecular Electronics*; John Wiley & Sons: Tauton, Somerset, 1992.
(7) Petty, M. C.; Bryce, M. R.; Bloor, D. *Introduction to Molecular Electronics*; Oxford University Press: New York, 1995.
(8) Balzani, V.; Credi, A.; Venturi, M. *Molecular Devices and Machines: A Journey into the Nanoworld*; Wiley-VCH: Weinhein, 2003.

Published on Web 02/10/2010

blocks that may be employed for the construction of such devices.[9−12]

One family of organic molecular materials with promising electronic properties identified to date is the phenylene−ethynylene oligomer (OPE).[13−20] The basic structure of OPE derivatives consists of a highly conjugated structure composed of alternating phenylene rings and acetylenic (C≡C) moieties (i.e., —(C_6R_4—C≡C—)$_n$). This skeleton provides a rigid, linear structure that supports a delocalized π electron system which in turn leads to fluorescent and electroluminescent properties,[21,22] as well as molecular wirelike features.[14,23,24] In the most general terms, the OPE structure can vary from two phenyl rings separated by a triple bond (tolan derivatives)[25−27] to oligomers,[22,28] or polymers[14] containing a high number of phenylene ethynylene repeat units. Oligomers of well-defined chemical composition are suitable for the construction of molecular electronic devices, with many convenient synthetic methods being available, rendering a wide variety of functional accessible.[29−31] However, even when working with chemically well-defined oligomeric structures, considerable care must be exercised to identify the extended molecular interactions and aggregation phenomena in the solid state; it is well-known that the extended molecular organization, as well as the nature of the contact between the molecule and solid interface, can play a significant role in modulating the final signal of the device arising from active molecular units since the intermolecular interactions can modify, magnify, or even create the response to external signals.[32−37] The methods and mechanisms available for assembly of molecular electronic candidates onto surfaces is therefore an area of considerable interest.

To date, OPE derivatives have been mainly ordered in two-dimensional arrays on solid surfaces by means of the self-assembly (SA) technique.[38] The SA method permits the fabrication of high quality thin (monolayer) films from suitably functionalized molecular materials through relatively simple protocols.[39,40] The most commonly explored SA systems have taken advantage of the strong interaction between gold and thiols.[41,42] However, this method presents several experimental disadvantages related to the instability of thiol groups[43] and also rather limits the number of metal−organic interfaces which can be analyzed. Thus, despite the undisputed success of thiol on gold SA films in developing much of the contemporary research in molecular electronics, a systematic study of different organic−metal contacts is of vital importance to determine the role that the interface plays in measurements of the conductivity of single molecules.[33,44]

In the Langmuir−Blodgett (LB) technique, assembly of molecular films is driven by an organization of the material at the air−water interface through the amphiphilic nature of the molecules that, on the one hand, permits its anchoring at the water surface and, on the other hand, facilitate a close-packed arrangement of the material by means of van der Waals interactions between neighboring molecules upon the compression process. Once the molecules are well-ordered at the air−water interface, the film can be transferred onto a solid support. Physisorbed LB films are very common (due to the large

(9) Wang, C.; Batsanov, A. S.; Bryce, M. R.; Martin, S.; Nichols, R. J.; Higgins, S. J.; Garcia-Suarez, V. M.; Lambert, C. J. *J. Am. Chem. Soc.* **2009**, *43*, 15647–15654.
(10) Kim, B.; Beebe, J. M.; Oliier, C.; Rigaut, S.; Touchard, D.; Kushmeric, J. G.; Zhu, X. Y.; Frisbie, C. D. *J. Phys. Chem. C* **2007**, *111*, 7521.
(11) Mahapatro, A. K.; Ying, J. W.; Ren, T.; Janes, D. B. *Nano Lett.* **2008**, *8*, 2131.
(12) Tour, J. M. *Chem. Rev.* **1996**, *96*, 537.
(13) Martin, R. E.; Diederich, F. *Angew. Chem., Int. Ed.* **1999**, *38*, 1350.
(14) Cui, X.; Primak, A.; Zarate, Z.; Tomfohr, J.; Sankey, O. F.; Moore, A. J.; Moore, T. A.; Gust, D.; Harris, G.; Lindsay, S. M. *Science* **2001**, *294*, 571.
(15) Bunz, U. H. F. *Chem. Rev.* **2000**, *100*, 1605.
(16) Richter, L. J.; Yang, C. S.-C.; Wilson, P. T.; Hacker, C. A.; van Zee, R. D.; Stapleton, J. J.; Allara, D. L.; Yao, Y.; Tour, J. M. *J. Phys. Chem. B* **2004**, *108*, 12547.
(17) Bunz, U. H. F. *Acc. Chem. Res.* **2001**, *34*, 988.
(18) Bunz, U. H. F. *Adv. Polym. Sci.* **2005**, *177*, 1.
(19) Huber, R.; Gonzalez, M. T.; Wu, S.; Langer, M.; Grunder, S.; Horhoiu, V.; Mayor, M.; Bryce, M. R.; Wang, C. S.; Jitchati, R.; Schonenberger, C.; Calame, M. *J. Am. Chem. Soc.* **2008**, *130*(3), 1080.
(20) Wu, S.; González, M. T.; Huber, R.; Grunder, S.; Mayor, M.; Schönenberger, D.; Calame, M. *Nat. Nanotechnol.* **2008**, *3*(9), 569.
(21) Arias, E.; Maillou, T.; Moggio, I.; Guillon, D.; Le Moigne, J.; Geffroy, B. *Synth. Met.* **2002**, *127*, 229.
(22) Arias-Marín, E.; Arnault, J. C.; Guillon, D.; Maillou, T.; Le Moigne, J.; Geffroy, B.; Nunzi, J. M. *Langmuir* **2000**, *16*, 4309.
(23) Donhauser, Z. J.; Mantooth, B. A.; Kelly, K. F.; Bumm, L. A.; Monnell, J. D.; Stapleton, J. J.; Price, D. W., Jr.; Rawlett, A. M.; Allara, D. L.; Tour, J. M.; Weiss, P. S. *Science* **2001**, *292*, 2303.
(24) Joo, S. H.; Jeong, M. Y.; Ko, D. H.; Park, J. H.; Kim, K. Y.; Bae, S. J.; Chung, I. J.; Jin, J. I. *Appl. Polym. Sci.* **2006**, *100*, 299.
(25) Smith, C. E.; Smith, P. S.; Thomas, R. L.; Robins, E. G.; Collings, J. C.; Dai, C. Y.; Scott, A. J.; Borwick, S.; Batsanov, A. S.; Watt, S. W.; Clark, S. J.; Viney, C.; Howard, J. A. K.; Clegg, W.; Marder, T. B. *J. Mater. Chem.* **2004**, *14*(3), 413.
(26) Pera, G.; Villares, A.; Lopez, M. C.; Cea, P.; Lydon, D. P.; Low, P. J. *Chem. Mater.* **2007**, *19*(4), 857.
(27) Tour, J. M.; Kozaki, M.; Seminario, J. M. *J. Am. Chem. Soc.* **1998**, *120*, 8486.
(28) Creager, S.; Yu, C. J.; Bamdad, C.; O'Connor, S.; MacLean, T.; Lam, E.; Chong, Y.; Olsen, G. T.; Luo, J.; Gozin, M.; Kayyem, J. F. *J. Am. Chem. Soc.* **1999**, *121*, 1059.
(29) Nguyen, P.; Yaun, Z.; Agocs, L.; Lesley, G.; Marder, T. B. *Inorg. Chim. Acta* **1994**, *220*, 289.
(30) Lydon, D. P.; Porres, L.; Beeby, A.; Marder, T. B.; Low, P. J. *New J. Chem.* **2005**, *15*, 4854.
(31) Wang, C. S.; Batsanov, A. S.; Bryce, M. R.; Sage, I. *Synthesis-Stuttgart* **2003**, *13*, 2089.
(32) Joachim, C.; Gimzewski, J. K.; Aviram, A. *Nature* **2000**, *408*(6812), 541.
(33) Lewis, P. A.; Inman, C. E.; Maya, F.; Tour, J. M.; Hutchison, J. E.; Weiss, P. S. *J. Am. Chem. Soc.* **2005**, *127*, 17421.
(34) Weibel, N.; Grunder, S.; Mayor, M. *Org. Biomol. Chem.* **2007**, *5*, 2343.
(35) Lindsay, S. M.; Ratner, M. A. *Adv. Mater.* **2007**, *19*, 23.
(36) Tour, J. M.; He, T. *Nature* **2008**, *453*, 54.
(37) Zhang, J.; Kuznetsov, A. M.; Medvedev, I. G.; Chi, Q.; Albrecht, T.; Jensen, P. S.; Ulstrup, J. *Chem. Rev.* **2008**, *108*, 2737.
(38) Bumm, L. A.; Arnold, J. J.; Cygan, M. T.; Dunbar, T. D.; Burgin, T. P.; Jones, L.II; Allara, D. L.; Tour, J. M.; Weiss, P. S. *Science* **1996**, *271*, 1705.
(39) Fendler, J. H. *Chem. Mater.* **2001**, *13*, 3196.
(40) Adams, D. M.; Brus, L.; Chidsey, C. E. D.; Creager, S.; Creutz, C.; Kagan, C. R.; Kamat, P. V.; Lieberman, M.; Lindsay, S.; Marcus, R. A.; Metzger, R. M.; Michel-Beyerle, M. E.; Miller, J. R.; Newton, M. D.; Rolison, D. R.; Sankey, O.; Schanze, K. S.; Yardley, J.; Zhu, X. *J. Chem. Phys. B* **2003**, *107*, 6668.
(41) Nuzzo, R. G.; Allara, D. L. *J. Am. Chem. Soc.* **1983**, *105*, 4481.
(42) Dhirani, A.; Zehner, R. W.; Hsung, R. P.; Guyot-Sionnest, P.; Sita, L. R. *J. Am. Chem. Soc.* **1996**, *118*, 3319.
(43) Tour, J. M.; Jones, L.II; Pearson, D. L.; Lamba, J. J. S.; Burgin, T. P.; Whitesides, G. M.; Allara, D. L.; Parikh, A. N.; Atre, S. V. *J. Am. Chem. Soc.* **1995**, *117*, 9529.
(44) Kushmerick, J. G.; Holt, D. B.; Yang, J. C.; Naciri, J.; Moore, M. H.; Shashidhar, R. *Phys. Rev. Lett.* **2002**, *89*, 086802.

flexibility in both the substrate material and the amphiphilic group of the assembled compound), although chemisorption can occur if there is a specific interaction between the molecule and the substrate. Recently, the LB method has received renewed interest as a process for the fabrication of thin films containing OPE derivatives[26,45−49] and provides a simple base from which to explore a very wide variety of organic−metal contacts (e.g., nitrile, amine, carboxylic acid, etc., on a wide variety of substrates Pt, Pd, Ag, etc.).[26,45−47,50−52]

OPE derivatives used to date for assembly into films by the LB technique have contained both a polar headgroup, which allows the monolayers to be stable at the air−liquid interface thanks to the polar headgroup−water interactions and an alkyl chain "tail" to provide stability to the monolayer thanks to the van der Waals interactions. However, from the point of view of the future molecular electronic applications of these materials, there is a remarkable advantage in using OPE derivatives without the supporting, but insulating, alkyl chain "tail", given that a direct connection between the conjugated ring and the gold tip of the scanning tunneling microscope is expected to facilitate smooth electrical transport. Prompted by this picture of the current landscape, we have now explored the film forming properties of 4-[4′-(phenylethynyl)-phenylethynyl] benzoic acid (BPEBA, Figure 1), an OPE derivative funtionalized with an acid group to facilitate its spreading and anchoring onto the water surface, but without an alkyl tail that could limit the conducting properties of the resulting films. BPEBA is shown to yield high quality films with promising electronic properties.

Experimental Section

Synthesis. *General Conditions*. All reactions were carried out under an atmosphere of nitrogen using standard Schlenk techniques. Nonaqueous solvents were purified and dried using an Innovative Technology SPS-400, or in the case of NEt_3 by distillation from KOH, and degassed before use. No special precautions were taken to exclude air or moisture during workup. The compounds $PdCl_2(PPh_3)_2$,[53] and 1-ethynyl-4(phenylethynyl)-benzene[54] were prepared by the literature methods. Other reagents were purchased and used as received. NMR spectra were recorded on Bruker Avance (^{1}H 400.13, ^{13}C 100.61, ^{31}P 161.98 MHz) or Varian Mercury (^{31}P 161.91 MHz) spectrometers from $CDCl_3$ solutions and referenced against solvent resonances.

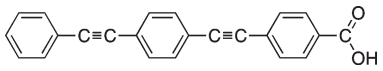

Figure 1. Chemical structure of the 4-[4-(phenylethynyl)-phenylethynyl] benzoic acid (BPEBA).

A suspension of 1-ethynyl-4(phenylethynyl)benzene (0.77 g, 3.81×10^{-3} mol), methyl iodobenzoate (0.93 g, 3.54×10^{-3} mol), $PdCl_2(PPh_3)_2$ (0.053 g, 7.60×10^{-5} mol), and CuI (0.014 g, 7.60×10^{-5} mol) in triethylamine (70 mL) was allowed to stir overnight. The ammonium salt formed was removed by filtration, and the solvent was removed from the filtrate to give crude 4-[4′-(phenylethynyl)-phenylethynyl] methyl benzoate, which was recrystallized from toluene/hexane. The ester was hydrolyzed in refluxing 1:1 aqueous ethanol (50 mL) containing sodium hydroxide (2.00 g, 5.00×10^{-2} mol). The volatiles were removed and 4-[4′-(phenylethynyl)-phenylethynyl] benzoic acid (BPEBA) obtained as a precipitate by treatment of the aqueous solution of the sodium salt with hydrochloric acid (2 M).

Film Fabrication. The films were prepared on a Nima Teflon trough with dimensions 720×100 mm^2, which was housed in a constant temperature (20 ± 1 °C) clean room. A Wilhelmy paper plate pressure sensor was used to measure the surface pressure (π) of the monolayers. The subphase was an aqueous (Millipore Milli-Q, resistivity 18.2 MΩ·cm) solution of NaOH whose pH was 9, which leads to ionization of the carboxylic group and further reduces the tendency for aggregation of the OPE. The solution containing the 4-[4′-(phenylethynyl)-phenylethynyl] benzoic acid (BPEBA) in a 2:1 hexane:ethanol solvent (both purchased from Aldrich and used as received; purity ≥99% and >99.5%, respectively) was delivered from a syringe held very close to the surface, allowing the surface pressure to return to a value as close as possible to zero between each addition. Hexane was employed as the spreading solvent since the BPEBA is not soluble in the common liquids used in the Langmuir−Blodgett technique. The use of ethanol in the spreading solvent serves to limit the formation of hydrogen-bonded carboxylic acid dimers and aggregates in solution prior to deposition. The spreading solvent was allowed to completely evaporate from the surface of the subphase over a period of at least 20 min before compression of the monolayer commenced at a constant sweeping speed of 0.02 nm^2/molecule·min. Under these experimental conditions, the isotherms were highly reproducible. Surface potential measurements were carried out using a Kelvin Probe provided by Nanofilm Technologie GmbH, Göttingen, Germany. During monolayer compression, $\pi-A$ and $\Delta V-A$ isotherms were recorded simultaneously.

The solid substrates used for the transferences were cleaned carefully as described elsewhere.[55,56] The monolayers were deposited at a constant surface pressure by the vertical dipping method, and the dipping speed was 6 mm/min. UV−vis spectra of the LB films were acquired on a Varian Cary 50 spectrophotometer and recorded using a normal incident angle with respect to the film plane. The fluorescence spectra were recorded by means of a Horiba-Jobin-Yvon Fluorolog 3-22 Tau-3 spectrofluorimeter. The RAMAN and SERS spectra were obtained using a Horiba Jobin Yvon LabRAM HR with an excitation wavelength of 633 nm. Silver islands (thickness 9.1 nm) were prepared in an Edwards model 306 vacuum coater from a resistively heated tungsten boat. The substrates were Menzel−Glaser glass

(45) Villares, A.; Lydon, D. P.; Porrès, L.; Beeby, A.; Low, P. J.; Cea, P.; Royo, F. M. *J. Phys. Chem. B* **2007**, *111*, 7201.
(46) Tang, Z. X.; Hicks, R. K.; Magyar, R. J.; Tretiak, S.; Gao, Y.; Wang, H. L. *Langmuir* **2006**, *22*, 8813.
(47) Villares, A.; Lydon, D. P.; Low, P. J.; Robinson, B. J.; Ashwell, G. J.; Royo, F. M.; Cea, P. *Chem. Mater.* **2008**, *20*, 258.
(48) Villares, A.; Martin, S.; Giner, I.; Diaz, J.; Lydon, D. P.; Low, P.; Cea, P. *Soft Matter* **2008**, *4*, 1508.
(49) Villares, A.; Lydon, D. P.; Robinson, B. J.; Ashwell, G.; Royo, F. M.; Low, P. J.; Cea, P. *Surf. Sci.* **2008**, *602*(24), 3683.
(50) Stapleton, J. J.; Daniel, T. A.; Uppili, S.; Carbarcos, O. M.; Naciri, J.; Shashidhar, R.; Allara, D. L. *Langmuir* **2005**, *21*, 11061.
(51) Love, J. C.; Wolfe, B. D.; Haasch, R.; Chabinyc, M. L.; Paul, K. E.; Whitesides, G. M.; Nuzzo, R. G. *J. Am. Chem. Soc.* **2003**, *125*, 2597.
(52) Rampi, M. A.; Whitesides, G. M. *Chem. Phys.* **2002**, *281*, 373.
(53) Clark, H. C.; Dixon, K. R. *J. Am. Chem. Soc.* **1969**, *91*(3), 596.
(54) Dirk, S. M.; Tour, J. M. *Tetrahedron* **2003**, *59*, 287.
(55) Cea, P.; Morand, J. P.; Urieta, J. S.; Lopez, M. C.; Royo, F. M. *Langmuir* **1996**, *12*, 1541.
(56) Martin, S.; Cea, P.; Lafuente, C.; Royo, F. M.; Lopez, M. C. *Surf. Sci.* **2004**, *563*, 27.

microscope slides cleaned in piranha solution for 30 min (3:1 97% H_2SO_4:30% H_2O_2), rinsed with deionized water, dried in a stream of N_2. During film deposition, the background pressure was maintained at 2×10^{-6} Torr, and the deposition rate (0.02 nm·s^{-1}) was monitored on an Edwards FTM7 quartz crystal film thickness monitor. After deposition, annealing was performed at 200 °C for 60 min in a nitrogen atmosphere.

The atomic force microscopy (AFM) imaging was performed with a multimode Nanoscope IIIA microscope (Digital Instruments, Veeco). The AFM tip was made of silicon with a resonant frequency of 285 kHz and a force constant of 42 N/m. All the images were recorded under ambient atmosphere at room temperature using tapping mode. The scanning rate was 1 Hz, and the amplitude set point was lower than 1 V. Cyclic voltammetry (CV) experiments were carried out in an electrochemical cell containing three electrodes. The working electrode consisted of a gold substrate with the deposited LB film, the counter electrode was a platinum sheet, and the reference electrode was Ag |AgCl| saturated KCl.

An Agilent STM running Picoscan 4.19 Software was used for all scanning tunneling microscopy (STM) and STM based electrical measurements. The tip potential is referred to as U_t. STM tips were freshly prepared for each experiment by etching of a 0.25 mm Au wire (99.99%) in a mixture of HCl (50%) and ethanol (50%) at +2.4 V. Gold films employed as substrates were purchased from Arrandee, Schroeer, Germany. These were flame-annealed at approximately 800−1000 °C with a Bunsen burner immediately prior to use. This procedure is known to result in atomically flat Au(111) terraces.[57]

Results and Discussion

The Langmuir−Blodgett technique (LB) was used to assemble the BPEBA molecules into thin, well ordered films. The protocol to fabricate true monolayers at the air−water interface was carefully designed and tested (see the Experimental Section) with the aim of decreasing the molecular forces between the BPEBA units which may lead to the formation of three-dimensional aggregates. The reproducible surface pressure and surface potential isotherms are shown in Figure 2.

With the purpose of analyzing in more detail the information provided by the $\pi-A$ isotherm, the compressibility coefficient, C_s, has been determined:[58]

$$C_s = -\frac{1}{A}\left(\frac{\partial A}{\partial \pi}\right)_T \quad (1)$$

By analyzing the $C_s-\pi$ curves, phase transitions can be detected in terms of changes in the slope. Furthermore, the compressibility modulus, K_s ($K_s = C_s^{-1}$), provides information about the phases and phase transitions of the monolayer according to the classification of Davies and Rideal.[59] Figure 3 shows the $C_s-\pi$ curve for the BPEBA monolayer at the air−water interface together with the Young modulus.

The surface pressure is zero in the $a-b$ region (Figure 2), which corresponds to the gas phase ($C_s > 0.085$ m/mN).[59]

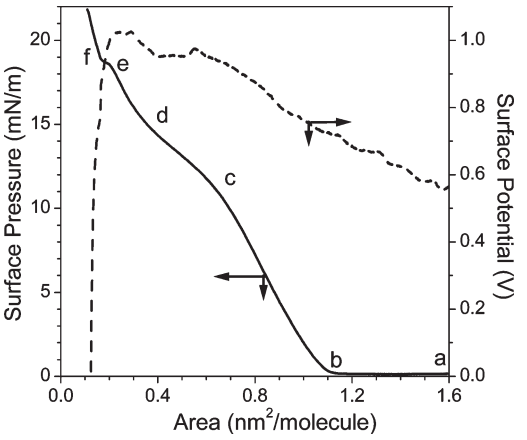

Figure 2. Surface pressure and surface potential versus area per molecule isotherms of BPEBA acid onto a NaOH aqueous subphase (pH 9).

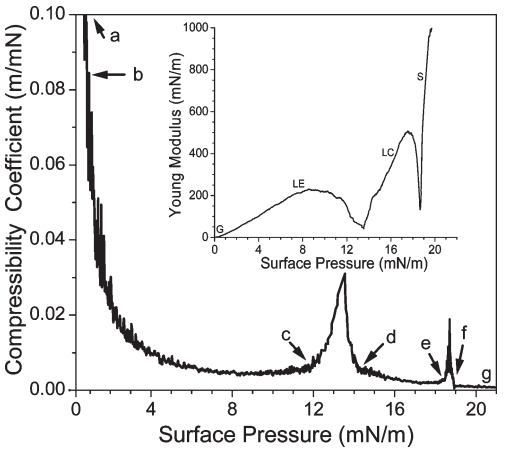

Figure 3. Compressibility coefficient (C_s) plotted as a function of the surface pressure (π) for the BPEBA monolayer at the air−water interface. The inset figure represents the Young modulus isotherm where the different phases of the monolayer have been indicated.

The lift-off in the isotherm appears at 1.10 nm^2/molecule (point b in Figure 2), with a monotonous increase of the surface pressure upon compression. The $b-c$ region in the isotherm corresponds to a liquid expanded (LE) phase according to the Young modulus values (see inset of Figure 3).[59] At point c in Figure 2 (0.60 nm^2, 12 mN/m), a change in the slope of the $\pi-A$ isotherm occurs, followed by a lower sheer region ($c-d$). This $c-d$ region is accompanied by a sharp symmetric peak in the $C_s-\pi$ graph, which is indicative of a phase transition, arguably, a liquid expanded−liquid condensed phase transition (LE-LC). At e (0.20 nm^2, 18.5 mN/m), the surface pressure increases again, accompanied by a drastic increase in K_s, whose values point out a liquid condensed phase (LC).[59] At 19 mN/m, there is a small plateau ($e-f$) that we have assigned to a liquid condensed−solid (LC-S) transition, which is followed by another sharp increase in the surface pressure upon compression, probably due to the fact that the monolayer is entering into the solid phase. It is noted at this point that $\Delta V-A$ isotherms are well-known to anticipate the phase changes a few angstroms before they are detected in the $\pi-A$ isotherms,[60]

(57) Haiss, W.; Lackey, D.; Sass, J. K. *J. Chem. Phys.* **1991**, *95*(3), 2193.
(58) Gaines, G. L. *Insoluble monolayers at liquid-gas interface*; Interscience Publisers. John Wiley & Sons: New York, 1966.
(59) Davies, J. T.; Rideal, E. K. *Interfacial Phenomena*; Academic Press: New York, 1963.
(60) Oliveira, O. N., Jr.; Bonardi, C. *Langmuir* **1997**, *13*, 5920.

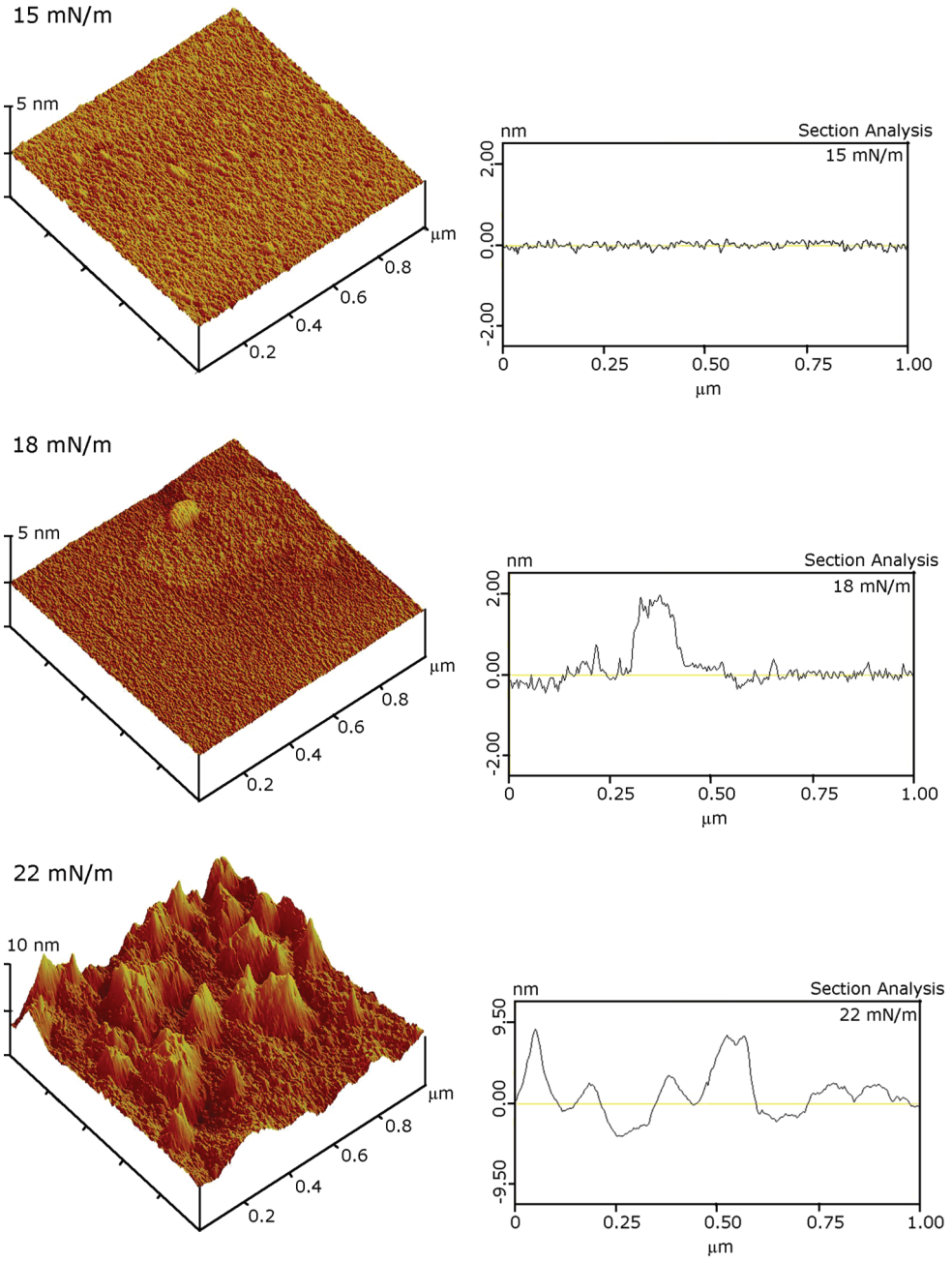

Figure 4. 3D views of AFM images (left) and section analysis profile (right) of a one layer LB film of BPEBA transferred onto freshly cleaved mica at the indicated surface pressures.

and this is the case as well in the isotherms shown in Figure 2. The sudden decrease of ΔV values at ca. 0.22 nm^2 is especially worthy of note. This decrease in ΔV values upon compression is consistent with a collapse of the monolayer, in which the dipole moments are randomly distributed in a three-dimensional arrangement of BPEBA molecules.

Langmuir monolayers were transferred onto solid substrates by the vertical dipping method with the hydrophilic substrates initially immersed in water. During the upstroke process, the deposition ratio is close to unity (≈ 0.99) for all the surface pressures of transference studied. However, during the immersion process, the transference ratio is close to zero; therefore, the deposition of BPEBA molecules is Z-type, resulting in the formation of noncentrosymmetric LB layers, which could be of interest at a later date for nonlinear optical applications.

The morphology of the transferred films was evaluated by atomic force microscopy (AFM). Monolayers of BPEBA were deposited onto freshly cleaved mica substrates at several surface pressures of transference. Some representative images and section analysis profiles are shown in Figure 4.

AFM images of BPEBA acid monolayers transferred at 15 mN/m show a homogeneous surface, in which the mica is wholly covered by the monolayer (lower surface pressures of transference show the presence of holes or incompletely covered surfaces). This result is indicative of a high surface coverage even at this relatively low surface pressure. The film roughness, calculated in terms

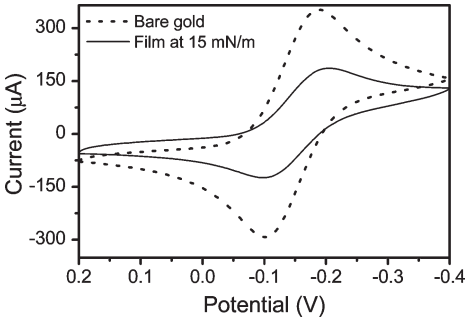

Figure 5. Cyclic voltammogram (CV) of a single-layer thick LB film of BPEBA deposited on a gold electrode at 15 mN/m surface pressure (solid line). The LB film deposited on the gold working electrode was immersed in aqueous solutions of 1 mM $Ru(NH)_6Cl_3$ and 0.1 M KCl, and CVs were recorded. The scan rate was 0.1 V/s at 20 °C, and the initial scan direction was negative. The surface area of the working electrode was 1 cm^2. An Ag|AgCl| saturated KCl reference electrode was employed, and the counter electrode was a Pt sheet. The dashed line shows the response of a bare gold electrode in the same solution.

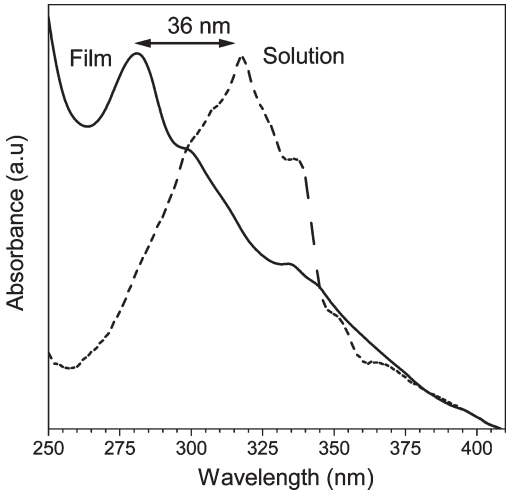

Figure 6. UV−vis spectrum of a one-layer film of BPEBA transferred at 15 mN/m onto a quartz substrate (solid line) and UV−vis spectrum of BPEBA solution in hexane (dotted line).

of the root mean squared (rms) is quite low, about 0.10 nm over areas of 1 μm^2. In contrast, monolayers deposited at a surface pressure of 18 mN/m give much less homogeneous films, which are characterized by the presence of higher irregular domains. The height of these domains is between 0.8 and 1.2 nm, likely indicating that some molecules are ejected from the film plane, in agreement with the data provided by the $\Delta V-A$ isotherm, giving rise to multilayer regions. Finally, the films transferred at 22 mN/m show a nonhomogeneous and irregular surface, which is a clear indication of the transference of three-dimensional structures. From these results, we concluded that the optimum surface pressure of transference is around 15 mN/m, for which a real monolayer free of three-dimensional defects and holes is deposited.

The OPE derivative used in this work lacks the alkyl chains that are commonly used to stabilize LB films by promoting strong van der Waals interactions between neighboring molecules and opens the question of whether the films prepared from BPEBA are well-packed. To address this point and obtain further information about the quality of the LB films that can be formed from BPEBA, Langmuir films of BPEBA were transferred onto gold electrodes initially immersed in the water subphase. The electrochemical current from a redox probe molecule in solution (ruthenium hexamide) at the electrode under controlled applied potential gives an indirect gauge of defect densities in thin films on surfaces.[61,62] Figure 5 shows the cyclic voltammogram (CV) obtained from aqueous solutions containing 1 mM $Ru(NH)_6Cl_3$ and 0.1 M KCl, using gold working electrodes modified by monolayer LB films deposited at 15 mN/m. For comparison, the electrochemical response of a bare gold electrode is shown. The peaks corresponding to the reduction and subsequent oxidation of the redox probe have significantly reduced their intensity for the LB film covered surface, which is indicative of passivation of the electrode and a relatively compact monolayer.

The optical properties of the transferred films offer additional insight into the molecular arrangement and degree of order within the film. A Langmuir film of BPEBA was transferred onto quartz substrates at 15 mN/m, and the UV−vis absorption spectrum was recorded (Figure 6). For the purpose of comparison, the UV−vis spectrum of BPEBA in hexane solution is also plotted.

The spectrum of the LB film shows a main band centered at 281 nm and a series of partially resolved absorption bands at 299 and 335 nm, while the solution spectrum presents a main peak centered at 317 nm with a shoulder at 336 nm, characteristic of the phenylene−ethynylene moiety.[63] The small features at longer wavelengths in the solution spectrum likely arise from dimers or other aggregates. The blue shift of 36 nm in the film spectrum with respect to that of the solution is attributable to the formation of two-dimensional H-aggregates. These aggregates are commonly found in LB films in which the chromophore has the main dipole transition moment arranged more or less along the amphiphile backbone, such as *trans*-stilbenes,[64,65] *trans*-azobenzenes,[66] hemicyanine derivatives,[67] squaraines,[68] and OPE derivatives.[26] It is also noted at this point that LB films of this compound incorporating an alkyl chain of six carbon atoms are characterized by a blue shift of 60 nm with respect to the solution.[45] This result indicates that the presence of alkyl chains has a significant effect on the optical behavior of the films and the arrangement of this family of compound in two-dimensional systems.

(61) Porter, M. D.; Bright, T. B.; Allara, D. L.; Chidsey, C. E. D. *J. Am. Chem. Soc.* **1987**, *109*, 3559.
(62) Cea, P.; López, M. C.; Martin, S.; Villares, A.; Pera, G.; Giner, I. *J. Chem. Educ.* **2009**, *86*(6), 723.
(63) Beeby, A.; Findlay, K.; Low, P. J.; Marder, T. B. *J. Am. Chem. Soc.* **2002**, *124*(28), 8280.
(64) Kaji, H.; Shimoyama, Y. *Jpn. J. Appl. Phys.* **2001**, *40*, 1396.
(65) Martin, S.; Cea, P.; Pera, G.; Haro, M.; Lopez, M. C. *J. Colloid Interface Sci.* **2007**, *308*, 239.
(66) Pedrosa, J. M.; Martín-Romero, M. T.; Camacho, L. *J. Phys. Chem. B* **2002**, *106*, 2583.
(67) Heeseman, J. *J. Am. Chem. Soc.* **1980**, *102*, 2166.
(68) Chen, H.; Law, K.-Y.; Whitten, D. G. *J. Phys. Chem.* **1996**, *100*, 5949.

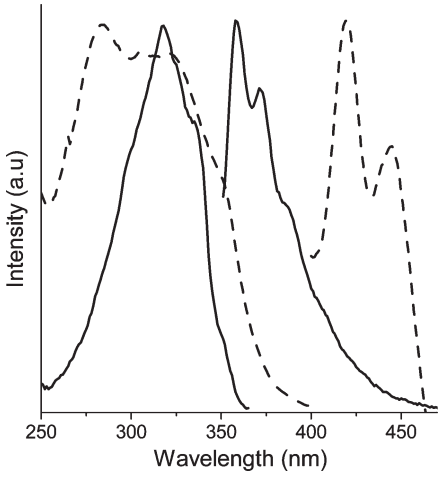

Figure 7. Normalized fluorescence excitation (left, λ_{em} = 400 nm) and emission (right, λ_{ex} = 372 nm) of BPEBA in hexane solution (solid lines) and in LB films transferred at 15 mN/m (dotted lines).

The 1,4-bis(phenylethynyl)benzene skeleton is highly fluorescent,[63] and excitation and emission fluorescence spectra from the LB monolayers of BPEBA are similar in profile to those of the parent material 1,4-bis(phenylethynyl)benzene[63,69] (Figure 7).

The excitation spectra shown in both cases (solution and LB film) are considerably broader and less well-defined than the emission spectra, due to the greater rotational freedom of the phenylene−ethynylene substructure in the ground state. In addition, no mirror image relationship between the excitation and emission spectra is observed due to the conformational changes that follow excitation. Comparing the spectra of the LB films with those of the solution, two main features can be identified. First, the LB absorption spectra are broader with respect to the solution spectra, which is likely to arise from the presence of intermolecular interactions and 2D H-aggregate formation.[46] Second, there is a significant Stokes shift in the LB emission spectra illustrating the emission from the aggregate. The low optical density of these deposited films means that this observed shift is not due to reabsorpion effects as sometimes observed in the fluorescence from bulk solid materials.

The similarity of the excitation and emission spectra of the BPEBA LB films and both BPEBA and the parent molecule 1,4-bis(phenylethynyl)benzene in solution strongly suggest that the BPEBA has been deposited on the substrate without chemical modification. To further verify the chemical nature of the surface adhered molecular material, we turned to surface-enhanced Raman spectroscopy (SERS), which is known to be a useful tool for structural studies of molecules deposited onto metallic solid substrates.[70−74] The Raman spectrum of BPEBA

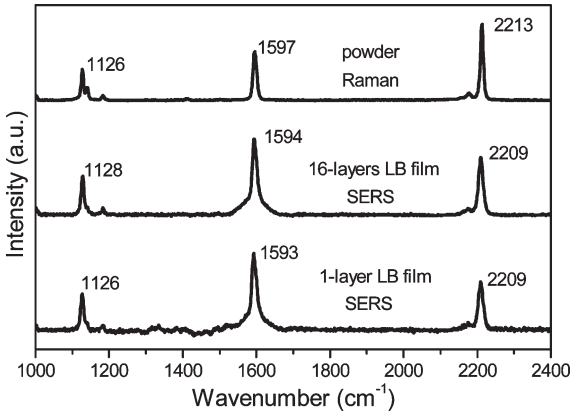

Figure 8. Raman spectrum of solid BPEBA and SERS spectra of 1-layer LB film and 16-layer LB film on silver islands.

(collected from powder samples of the pure solid material using a Raman microscope) and SERS spectra of both 1-layer and 16-layer LB films deposited on silver mirrors are depicted in Figure 8.

The Raman spectrum of the solid compound shows three major vibrational bands centered at 1126, 1597, and 2213 cm^{-1}. The highest wavenumber band is associated with the localized vibrational motion of the acetylene groups. The band at 1597 cm^{-1} is assigned to the symmetric stretch of the three aromatic rings along the long axis of the molecule, and the one at 1126 cm^{-1} is due to a symmetric C−H bending mode.[75] There are only minor band shifts and differences in intensity observed in the SERS spectra, and these are indicative of the differences in molecular environment between the powder and the adsorbate which leads to variations in the polarizability tensor of the deposited molecules.[76] When an adsorbate is chemically bonded to the solid surface, significant changes are observed between the bulk and SERS spectra characterized by peak shifts of 100 cm^{-1} or more;[74] however, physisorption results in only small variations in the band position and relative intensities.[77] In the present case, the small shift to lower wavenumbers in the spectra of the LB films with respect to the pure compound indicates that the BPEBA molecules are physisorbed to the silver substrate, i.e. the interaction between the BPEBA and the substrate is weak.

The electrical properties of these LB films were investigated with scanning tunnelling microscopy (STM). For these STM measurements, BPEBA monolayers were deposited at 15 mN/m onto Au(111). Current−voltage ($I-V$) curves were recorded and averaged from multiple scans (400 scans) recorded for different substrates and at different locations on each substrate to ensure the reproducibility of the results. Moreover, before recording $I-V$ curves, it is necessary to know the tip−substrate distance (s), in order to position the tip sufficiently above the monolayer

(69) Greaves, S. J.; Flynn, E. L.; Futcher, E. L.; Wrede, E.; Lydon, D. P.; Low, P. J.; Rutter, S. R.; Beeby, A. *J. Phys. Chem. B* **2006**, *110*, 2114.
(70) Moskovits, M. *Rev. Mod. Phys.* **1985**, *57*, 783.
(71) Jennings, C. A.; Kovacs, G. J.; Aroca, R. F. *Langmuir* **1993**, *9*, 2151.
(72) Wu, Y.; Zhao, B.; Xu, W.; Liw, B. *Langmuir* **1999**, *15*, 4625.
(73) Haro, M.; Ross, D. J.; Oriol, L.; Gascón, I.; Cea, P.; López, M. C.; Aroca, R. F. *Langmuir* **2007**, *23*(4), 1804.
(74) Patterson, M. L.; Weaver, M. J. *J. Phys. Chem.* **1985**, *89*, 5046.
(75) Beeby, A.; Findlay, K. S.; Low, P. J.; Marder, T. B.; Matousek, P.; Parker, A., W.; Rutter, S. R.; Towrie, M. *Chem. Commun.* **2003**, *19*, 2406.
(76) Iliescu, T.; Irimine, F. D.; Bolboaca, M.; Paisz, C.; Kiefer, W. *Vib. Spectrosc.* **2002**, *29*, 251.
(77) Vo-Dinh, T. *Trends Anal. Chem.* **1998**, *17*, 557.

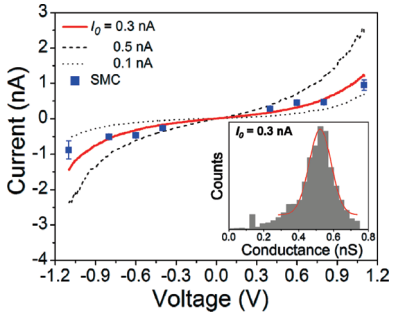

Figure 9. $I-V$ curves of single layer LB films of BPEBA transferred onto Au(111) at 15 mN/m using several set-point parameters: 0.1 nA (s = 1.96 nm) (dotted line); 0.3 nA (s = 1.80 nm) (solid line); and 0.5 nA (s = 1.72 nm) (dashed line). An $I-V$ curve constructed from single molecule conductance values obtained using the $I(s)$ method is also shown (blue squares). The error bars represent the standard deviation. U_t = 0.6 V. The inset graph shows the conductance histogram built by adding all the experimental data from −0.4 to 0.4 V for each $I-V$ curve obtained at U_t = 0.6 V and I_0 = 0.3 nA. The red solid line is the Gaussian fit.

and hence to avoid penetration of the STM tip into the film. To achieve this purpose, a careful calibration of the tip-to-substrate distance is required. The set-point parameters of the STM ($I_0 \equiv$ "set point current" and $U_t \equiv$ "tip bias") can be converted to an absolute gap separation (s)[78−80] according to the equation:

$$s = \frac{\ln(G_0 U_t / I_0)}{\mathrm{d}\ln(I)/\mathrm{d}s} \qquad (2)$$

where d ln(I)/ds was typically on the order of 6.65 ± 1.28 nm^{-1} and G_0 ($G_0 = 2e^2/h$ = 77.4 μS) is the conductance quantum.

Figure 9 shows $I-V$ curves obtained for a single layer BPEBA LB film using several set-point parameters (U_t = 0.6 V and I_0 = 0.1, 0.3, and 0.5 nA) which give different initial tip−substrate distances according to eq 2 (1.96, 1.80, and 1.72 nm, respectively, with the molecule length being 1.91 nm according to molecular models, Chem 3D). For statistical analysis, a histogram was constructed (for the set-point parameters U_t = 0.6 V and I_0 = 0.3 nA) by adding all the experimental data from −0.4 to 0.4 V (the linear region in the $I-V$ curve) for each curve and fitted by a Gaussian function (inset of Figure 9). In addition, Figure 9 also shows an $I-V$ curve constructed from single molecule conductance (SMC) values for BPEBA obtained using the $I(s)$ method at eight different bias voltage values. A description of the $I(s)$ technique can be found in the literature;[81,82] it has been widely employed to determine single molecule conductance.[79,80] When the set-point parameters are 0.3 nA and 0.6 V (tip−substrate distance of 1.80 nm), the $I-V$ curve for the LB film is practically the same as the one constructed from single molecule conductance values (Figure 9). Since the curve using these set-point parameters (0.3 nA and 0.6 V) coincides with the SMC-curve, it can be concluded that using these parameters the STM tip probes the conductance of a single BPEBA molecule embedded in the LB film. Presumably under these conditions, the STM tip is located right above the LB film and sufficiently strongly electronically coupled to a single molecule. Meanwhile, for 0.5 nA set-point current (s = 1.72 nm) the $I-V$ curve lies above that for a single molecule, so in this case the tip either probes conductance through more than a single molecule in the LB film and/or the tip penetrates inside the monolayer leading to a conductance increase. On the other hand, for a set-point current of 0.1 nA (s = 1.96 nm), the conductance decrease below the single molecule value, due to an increased gap between the tip and the LB film.

The profile of all the $I-V$ curves is nearly symmetrical in spite of the inherent asymmetry of the molecule; the oligomeric moiety has a carboxylic acid group on only one end of the molecule. Such behavior is anticipated as the molecule in this case is simply an amphiphilic electron-donating wire and does not possess the features of molecules (e.g., donor−acceptor moieties) which have shown strong rectifying (molecular diode) characteristics.[83−86] This nonrectifying behavior reported here has been previously seen for similar OPE derivatives.[47,87,88]

The $I-V$ curves for the LB films and those determined from single molecular conductance measurements are similar despite the different molecular surroundings in the two cases; in the LB film, the molecule is packed together with neighboring BPEBA molecules, while no such neighbors exist for the SMC determinations. This indicates that in the STM configuration intermolecular electron hopping does not significantly enhance the junction transport characteristics. The presence of neighboring π systems does not greatly influence the STM determined molecular conductance in spite of the existence of intermolecular interactions and aggregate formation (H-aggregates) in the LB films (as has been demonstrated by UV−visible and fluorescence spectroscopy).

Conclusions

A 1,4-bis(phenylethynyl)benzene derivative has been synthesized and assembled into well-packed monolayer films on a variety of substrates by means of the Langmuir−Blodgett technique. Langmuir films of BPEBA

(78) Haiss, W.; Wang, C.; Grace, I.; Batsanov, A. S.; Schiffrin, D. J.; Higgins, S. J.; Bryce, M. R.; Lambert, C. J.; Nichols, R. J. *Nat. Mater.* **2006**, *5*, 995.
(79) Haiss, W.; Martín, S.; Leary, E.; van Zalinge, H.; Higgins, S. J.; Bouffier, L.; Nichols, R. J. *J. Phys. Chem. C* **2009**, *113*, 5823.
(80) Sedghi, G.; Sawada, K.; Esdaile, J. L.; Hoffmann, M.; Anderson, H. L.; Bethell, D.; Haiss, W.; Higgins, S. J.; Nichols, R. J. *J. Am. Chem. Soc.* **2008**, *130*, 8582.
(81) Haiss, W.; van Zalinge, H.; Higgings, S. J.; Bethell, D.; Höbenreich, H.; Schiffrin, D. J.; Nichols, R. J. *J. Am. Chem. Soc.* **2003**, *125*, 15294.
(82) Haiss, W.; Nichols, R. J.; van Zalinge, H.; Higgins, S. J.; Bethell, D.; Schiffrin, D. J. *Phys. Chem. Chem. Phys.* **2004**, *6*, 4330.
(83) Ashwell, G. J.; Gandolfo, D. S. *J. Mater. Chem.* **2001**, *11*, 246.
(84) Ashwell, G. J.; Sambles, J. R.; Martin, A. S.; Parker, W. G.; Szablewski, M. *J. Chem. Soc. Chem. Commun.* **1990**, 1374.
(85) Baldwin, J. W.; Amaresh, R. R.; Peterson, I. R.; Shumate, W. J.; Cava, M. P.; Amiri, M. A.; Hamilton, R.; Ashwell, G. J.; Metzger, R. M. *J. Phys. Chem. B* **2002**, *106*, 12158.
(86) Martin, A. S.; Sambles, J. R.; Ashwell, G. J. *Thin Solid Films* **1992**, *210*, 313.
(87) Reichert, J.; Ochs, R.; Beckman, D.; Weber, H. B.; Mayor, M.; Löhneysen, H. v. *Phys. Rev. Lett.* **2002**, *88*(17), 176804.
(88) Ashwell, G. J.; Urasinska, B.; Tyrrell, W. D. *Phys. Chem. Chem. Phys.* **2006**, *8*, 3314.

were prepared at the air−water interface and characterized by surface pressure and surface potential vs area per molecule isotherms, which demonstrate that this molecule can form true monolayers at the air−water interface. The LB film was transferred onto solid substrates with a Z-type deposition with a transfer ratio close to 1. The morphology of the deposited films was analyzed by means of AFM revealing the formation of highly homogeneous films free of holes and three-dimensional defects for surface pressures of 15 mN/m. A hypsochromic shift of the absorption spectrum of the LB films of 36 nm with respect to the spectrum of a hexane solution of BPEBA indicates that two-dimensional H-aggregates are formed. The fluorescent properties of the thin films were evaluated, with fluorescence spectra showing similar features to the parent compound. Raman and SERS studies reveal that the BPEBA molecules are physisorbed onto a metallic silver surface. Electrical characteristics of the LB films on gold substrates were determined by positioning a gold STM tip sufficiently above the monolayer as determined from calibration of the tip-to-substrate distance. $I-V$ curves of the LB film were recorded using different setpoint parameters and then compared with $I-V$ curves constructed from single molecule conductance values obtained by the $I(s)$ technique. $I-V$ curves are symmetrical in spite of the asymmetric contacts of the molecule with respect to the tip and the substrate. These measurements show that BPEBA exhibits nonrectifying molecular wirelike characteristics.

Acknowledgment. The authors are grateful for financial assistance from Ministerio de Educación y Ciencia (MEC) from Spain and fondos FEDER in the framework of the projects CTQ2006-05236 and CTQ2009-13024 (A.V., G.P., and P.C.) as well as to DGA for its support through the interdisciplinary project PM079/2006 (A.V., A.B., P.J.L., and P.C.). We also thank ONE NorthEast for financial support through the Durham UIC Nanotechnology (A.B., P.J.L.) and the EPSRC for award of a Leadership Fellowship (P.J.L.). R.J.N acknowledges support by EPSRC under grant EP/C00678X/1 (Mechanisms of Single Molecule Conductance) A.V. and G.P. acknowledge their FPU studentships. S.M. acknowledges his Juan de la Cierva contract from Ministerio de Ciencia e Innovación (Spain), and P.C. is thankful for the award of an MEC grant for a research stay at Durham University. Finally, we thank Dr. C. Pearson and Prof. M. C. Petty from Durham University for the preparation of the silver substrates and useful discussions.